Nat Hazards (2013) 68:745–762
DOI 10.1007/s11069-013-0646-6

ORIGINAL PAPER

A formation model for debris flows in the Chenyulan River Watershed, Taiwan

Bin Yu · Li Li · Yufu Wu · Shengming Chu

Received: 7 December 2012 / Accepted: 13 March 2013 / Published online: 23 March 2013
© Springer Science+Business Media Dordrecht 2013

Abstract Many debris flows were triggered in the Chenyulan River Watershed in Taiwan in a rainstorm caused by the Typhoon Toraji. There are 117 gullies with a significant steep topography in the catchment. During this Typhoon, debris flows were initiated in 43 of these gullies, while in 34 gullies, it was not certain whether they have occurred. High-intensity short-duration rainfall was the main triggering factor for these gully type debris flows which are probably entrained by a "fire hose" mechanism. Previous research identified 47 factors related to topography, geology, and hydrology, which may play a role in the formation of gully type debris flows. For a better understanding of the probability of the formation of debris flows, it is proposed to represent the factors related to topography, geology, and hydrology by one single factor. In addition to the existing topographic and geological factor, a normalized critical rainfall factor is suggested with an effective cumulative precipitation and a maximum hourly rainfall intensity. In this paper, a formation model for debris flows is proposed, which combines these topographic, geological, and hydraulic factors. A relationship of these factors with a triggering threshold is proposed. The model produces a good assessment of the probability of occurrence of debris flows in the study area. The model may be used for the prediction of debris flows in other areas because it is mostly based on the initiation mechanisms and not only on the statistical analyses of a unique variety of local factors. The research provides a new and exciting way to study the occurrence of debris flows initiated by a "fire hose" mechanism.

B. Yu (✉)
State Key Laboratory of Geohazard Prevention and Geoenvironment Protection, Chengdu University of Technology, Chengdu 610059, China
e-mail: drbinyu@yahoo.com

L. Li
Southwest Geotechnical and Design Institute of China Nuclear Industry, Chengdu 610061, China

Y. Wu
Emergent Geohazards Center of Jiangxi Province, Nanchang 330025, China

S. Chu
Southwestern Architectural Design Institute Co. Ltd, Chengdu 610081, China

Keywords Formation model · Debris flow · Fire hose · Typhoon Toraji · Chenyulan River Watershed

1 Introduction

Many debris flows were triggered in the Chenyulan River Watershed in Taiwan in a rainstorm caused by the Typhoon Toraji. Most of these debris flows were gully type debris flows (Chen et al. 2005; Chen 2007). Gully type debris flows are dangerous and cause enormous risks. For example, the debris flows in Venezuela in 1999 with 15,000 deaths (Lopez et al. 2003) and the debris flows in China in 2010 causing 1744 casualties (Yu et al. 2010) are all gully type debris flows. Gully type debris flows differ from the so-called unconfined "hill slope debris flows" (VanDine 1985). Gully type debris flows take place in areas with significant gully topography (Liu et al. 2009). The gully type debris flows in the study area were triggered most of the time by flash floods (Chen et al. 2012) causing a so-called "fire hose" effect (Godt and Coe 2007). The fire hose effect is caused by the entrainment of material due to high shear stresses induced by a concentrated flow of water, as if the material had been washed away by a "fire hose" (Johnson and Rodine 1984; Coe et al. 1997; Griffiths et al. 2004).

To mitigate and prevent hazards induced by debris flows and related risks, one must understand the formation of these in order to make reliable forecasts. Many factors are related to the occurrence of debris flows like the basin gradient, the percentage of basin area with slopes greater than or equal to 30 %, basin ruggedness, additional measures of gradient, slope aspect, rainfall intensity, and soil properties, including the clay percentage, the percentage of organic matter, the soil granulometry and sorting, and the soil liquid limit. These were selected as the strongest determining factors for debris flow response in the forest fire burned basins of the Intermountain West (Cannon et al. 2010). The authors identified four groups of variables related to the occurrence of debris flows in burned basins: topography, degree of burning, soil properties, and rainfall variables.

Liu et al. (2009) among others stated that there are three groups of factors playing a major role in the formation of ordinary gully type debris flows. They are related to topography, geology, and hydrology. The topographical factors include watershed area, channel length, elevation difference, average slope, slope curvature, and a form factor (Lin et al. 2002; Lin 2009; Lan et al. 2004; Catani et al. 2005; Chang and Chao 2006; Chang 2007; Lu et al. 2007; Lee and Pradhan 2007; Chang and Chien 2007; Tiranti et al. 2008; Tunusluoglu et al. 2008; Ranjan et al. 2004; Akgun et al. 2008). The geological factors include among others lithology, soil type, fault length, distance to fault, and landslide area (Lin et al. 2002; Ohlmacher and Davis 2003; Lan et al. 2004; Catani et al. 2005; Lu et al. 2007; Lee and Pradhan 2007; Tiranti et al. 2008; Ranjan et al. 2004; Akgun et al. 2008). The hydrological factors include among others rainfall intensity, daily rainfall, cumulative rainfall, and antecedent rainfall (Chang and Chao 2006; Chang 2007; Lee and Pradhan 2007; Chang and Chien 2007; Tiranti et al. 2008). These factors were obtained from statistical correlation analyses of debris flow occurrences with topographic, geological, and hydrological aspects. Because of the uniqueness of these characteristics in each area, the correlation structure found in one area is not valid in other areas. This is why all these studies show so many different factors related to debris flow occurrence. It is therefore difficult to obtain a unique universal relationship between debris flows and topographic, geological, and hydrological characteristics. Past research revealed more than 47 factors related to debris flows (Lee 2006). The formation of debris flows will be much more predictable when topography, geology, and hydrology can be reduced to one single factor.

By focusing on the study of the process mechanisms, one can find significant and probably more general relationships between debris flow formation and the topographic, geological, and hydrological factors. In our case, they are the flash floods in large and steep channels which cause a so-called "fire hose" effect eroding especially the small size sediments (Godt and Coe 2007) leading to the formation of debris flows. So the major topographic, geological, and hydrological factors must refer to steep channels, small grain sizes of the sediments, and the development of large flash floods.

Yu et al. (2011) and Li (2012) proposed a topographic factor to describe the role of topography in the formation of debris flows triggered by the flash flood in channels. Yu et al. (2012) suggested a geological factor to represent the role of geology in the formation of this kind of debris flows. Shieh et al. (2009), Wu et al. (1990), and Tan and Han (1992) used the 1-h or 10-min rainfall intensity and effective cumulative precipitation to predict this kind of debris flows. These studies formed the base to analyze the formation of debris flows of 2001 in the Chenyulan River Watershed, which were triggered by flash floods in channels, using only 3 factors related to topography, geology, and hydrology. One critical parameter is derived from these three dimensionless factors in order to predict the occurrence of debris flows triggered by a "fire hose" mechanism.

2 The debris flow development in the Chenyulan River Watershed, Taiwan, during the Typhoon Toraji in 2001

Debris flows in the Chenyulan River Watershed were first reported during the Typhoon Wayne on August 22, 1986. During Typhoon Herb on July 29, 1996, debris flows occurred in more than 32 gullies (Lin et al. 2003; Jan and Chen 2005). The Chi–Chi earthquake ($ML = 7.3$), with a focal depth of 8.0 km, was triggered by reactivation of the Chelungpu fault in central Taiwan on September 21, 1999. This earthquake triggered many large landslides in central Taiwan (Kaima et al. 2000). Consequently, a great deal of loose sediments was produced, which in turn promoted heavy debris flows during subsequent typhoons and heavy rains. The most outstanding example was a large debris flow causing the deaths of more than 240 people during the Typhoon Toraji on July 30, 2001 (Lin et al. 2003). The rainfall threshold for debris flow initiation was significantly lower after the earthquake and recovered gradually in subsequent years (Shieh et al. 2009). The Typhoon Toraji, which occurred 2 years after the Chi–Chi earthquake, had a maximum rainfall intensity of 140 mm/h, a total rainfall of 700 mm, and a duration of 15 h in central and east Taiwan. It resulted in a severe debris flow development in the Chenyulan River Watershed (Lin et al. 2003).

Chen (2007) investigated after the Typhoon Toraji 117 gullies in the Chenyulan River Watershed with significant gully topography using SPOT images. She found debris flows in 65 out of a total of 117 surveyed gullies. Lin et al. (2003) used also SPOT images and carried out field investigations as well. He indentified debris flows in 55 out of the 117 gullies. The differences between the two studies are not only the number of debris flows, but also the uncertainty about the presence of debris flows in some gullies. In 43 cases, both studies agreed on the presence of debris flows in gullies, and in 40 cases, the two references agreed on the absence of debris flows, which means the presence of debris flows is uncertain in 34 gullies, because of the different judgment by both studies. Here, we define the occurrence of debris flows in the Chenyulan River Watershed during the

Typhoon Toraji as "Yes" or "No" if the judgment of the two studies is consistent and as "uncertain" in case of a contrary decision of the two references (see Table 1; Fig. 1).

The Chenyulan River is a main branch of the Chuo-Shui River, which is one of the three large rivers of Taiwan. The watershed lies in Central Taiwan and covers an area of 449 km^2. The river with a total length of 42 km flows in a south–north direction (Fig. 1). The junction with the Chuo-Shui River lies at an altitude of 310 m. The highest peaks in the catchment have altitudes between 2,500 and 3,000 m. The channel gradients in the upstream part of the gullies are mostly more than 20°. These are suitable topographic conditions for debris flow outbreaks.

The four lithological units of the Chenyulan River Watershed are as follows: quartz sandstones alternated with hard shales, hard shales alternated with quartz sandstones, slates and siltstones interbedded with shales. The Chenyulan River follows closely the Chenyulanchi fault line. Some other faults can be found in the study area (Chen et al. 2005; Bai 2007; see Fig. 2; Table 1).

The 32 debris flows which were triggered during the typhoon Herb in 1996 arose mainly by lateral and vertical erosion along the gully bed. Only a few landslides on steep and moderate slopes have been detected, which did not contribute to the debris flow development. Loose debris sediments were originally deposited in gully beds and these produced also during the Typhoon Toraji debris flows by severe and deep bed erosion. But also in areas without significant gully topography, the so-called slope debris flows (VanDine 1985; Lin et al. 2003) could develop in the original loose debris material. These slope debris flows are not considered in this study.

Long-duration rainfall such as produced by the Typhoon Herb in 1996 (more than 48 h), the Typhoon Midulle in 2004 (more than 48 h), and the Typhoon Morakot in 2009 (72 h) is the main cause for the development of large landslides in the study area (Chen et al. 2012). Short-duration high-intensity rainfall is the main inducing factor for the development of gully type debris flows with a "fire hose" mechanism like the Typhoon Toraji (duration 15 h; maximum intensity 140 mm/h) (Chen et al. 2012).

The Chenyulan River Watershed, located at some 12 km east of the epicenter, experienced 400–600 cm/s^2 of ground acceleration during the Chi–Chi earthquake, which caused large-scale rock fracturing and landslides (Lin et al. 2003). Huang and Li (2009) pointed out that in the Wenchuan earthquake area (Sichuan Provence, China), the co-seismic landslides are mainly concentrated within a distance of 7 km from the triggering fault. A second zone at a distance between 7 and 11 km from the fault was distinguished with a medium landslide density and a third effected zone with the lowest landslide density at a distance of more than 11 km from the fault. Since the Chelungpu fault, which triggered the Chi–Chi earthquake, is about 15–45 km away from the study area, the distance from the fault must have only a slight differential effect on the landslide density distribution in the study area. Therefore, the effect of the Chi–Chi earthquake is assumed to be the same throughout the study area.

3 The formation factors of debris flows with a "fire hose" mechanism

3.1 The topographic factor

Generally, the catchment of a debris flow is subdivided into a formation or source section, a transport or passing section, and a deposition section. The topographical factors influence in different ways the processes in these three sections of the catchment. In this study, we

Table 1 Parametric values related to different debris flow forming factors and the presence of debris flows in gullies of the Chenyulan River Watershed

No.	Lithology	*T*	*G*	*R*	*P*	Debris flow[a]	Debris flow[b]	Debris flow[c]
1	EO[1]	0.110	7.13	0.88	0.212	Yes	Yes	Yes
2	EO	0.201	7.13	0.857	0.233	Yes	Yes	Yes
3	EO	0.097	7.13	0.839	0.197	Yes	Yes	Yes
4	EO	0.135	6.84	0.832	0.213	Yes	Yes	Yes
5	EO, OM[2]	0.235	6.25	0.795	0.238	Yes	Yes	Yes
6	OM	0.257	5.65	0.785	0.252	Yes	Yes	Yes
7	EO, OM	0.174	6.24	0.787	0.222	Yes	Yes	Yes
8	OM	0.268	5.65	0.775	0.25	Yes	Yes	Yes
9	OM	0.156	5.65	0.777	0.225	Yes	Yes	Yes
10	OM	0.405	5.65	0.785	0.276	Yes	Yes	Yes
11	EO, OM	0.261	6.25	0.799	0.244	Yes	No	Uncertain
12	EO	0.246	6.84	0.734	0.212	Yes	No	Uncertain
13	EO, OM	0.194	6.25	0.763	0.22	No	No	No
14	OM	0.145	5.89	0.751	0.211	No	No	No
15	OM	0.158	5.89	0.737	0.21	No	No	No
16	EO	0.240	7.13	0.709	0.2	No	No	No
17	EO	0.158	7.13	0.694	0.18	No	No	No
18	OM	0.340	5.89	0.68	0.226	Yes	No	Uncertain
19	EO	0.297	7.13	0.666	0.196	Yes	No	Uncertain
20	EO	0.385	7.13	0.641	0.198	Yes	No	Uncertain
21	EO	0.155	7.13	0.883	0.228	Yes	Yes	Yes
22	EO	0.152	7.13	0.93	0.239	No	Yes	Uncertain
23	EO, OM	0.096	5.86	0.774	0.2	Yes	Yes	Yes
24	EO, OM	0.206	6.05	0.786	0.233	Yes	Yes	Yes
25	EO	0.165	6.42	0.74	0.204	Yes	Yes	Yes
26	EO	0.295	6.85	0.713	0.214	Yes	Yes	Yes
27	OM	0.322	5.89	0.624	0.205	No	No	No
29	EO	0.242	7.13	0.607	0.171	No	No	No
30	EO	0.315	7.13	0.573	0.17	Yes	No	Uncertain
31	EO, OM	0.192	6.51	0.55	0.155	No	No	No
32	EO	0.164	7.13	0.567	0.148	No	No	No
33	EO, OM	0.411	6.51	0.553	0.181	Yes	No	Uncertain
34	OM	0.329	5.65	0.557	0.187	Yes	Yes	Yes
35	OM	0.249	5.65	0.521	0.166	No	No	No
36	EO, OM	0.349	6.51	0.557	0.177	No	Yes	Uncertain
37	EO	0.210	7.13	0.514	0.141	No	No	No
38	EO	0.167	7.13	0.535	0.14	No	No	No
39	EO	0.310	7.13	0.547	0.162	No	No	No
40	EO	0.361	6.84	0.576	0.18	No	No	No
41	OM	0.218	5.65	0.594	0.184	No	Yes	Uncertain
42	OM	0.194	5.65	0.586	0.177	No	No	No
43	EO	0.097	6.84	0.57	0.137	No	Yes	Uncertain

Table 1 continued

No.	Lithology	*T*	*G*	*R*	*P*	Debris flow[a]	Debris flow[b]	Debris flow[c]
44	OM	0.178	5.65	0.628	0.187	No	Yes	Uncertain
45	EO, OM	0.193	6.25	0.63	0.181	No	Yes	Uncertain
46	EO	0.317	7.13	0.585	0.174	No	Yes	Uncertain
47	EO	0.461	7.13	0.593	0.19	No	Yes	Uncertain
48	EO	0.274	6.84	0.603	0.178	No	No	No
49	EO	0.316	7.13	0.588	0.175	No	No	No
50	EO	0.387	7.13	0.61	0.189	No	No	No
51	EO	0.423	6.84	0.509	0.164	No	No	No
53	EH[3]	0.262	8.04	0.4	0.108	No	No	No
54	EH	0.191	8.04	0.41	0.104	No	No	No
55	EH	0.211	8.37	0.396	0.1	Yes	No	Uncertain
56	MS[4]	0.181	4.65	0.542	0.178	Yes	Yes	Yes
57	EO, EH	0.217	7.75	0.463	0.122	No	No	No
58	EH	0.210	8.37	0.459	0.116	No	No	No
60	EH	0.373	8.37	0.316	0.09	No	No	No
61	MS	0.168	4.65	0.454	0.147	Yes	No	Uncertain
62	EH	0.266	8.04	0.356	0.096	No	No	No
64	MS,EH	0.193	6.51	0.372	0.105	No	No	No
65	MS	0.419	4.46	0.562	0.224	Yes	Yes	Yes
66	MS	0.200	4.46	0.481	0.165	No	No	No
67	MS	0.304	4.65	0.524	0.191	Yes	Yes	Yes
68	MS	0.328	4.65	0.554	0.206	Yes	Yes	Yes
69	MS	0.174	4.32	0.473	0.16	Yes	Yes	Yes
70	MS	0.152	4.65	0.481	0.153	Yes	Yes	Yes
71	MS	0.083	4.65	0.492	0.139	No	No	No
72	MS	0.172	4.65	0.485	0.158	Yes	Yes	Yes
73	MS	0.315	4.65	0.465	0.171	No	No	No
74	MS	0.278	4.65	0.475	0.17	No	No	No
75	MS	0.307	4.65	0.474	0.173	No	Yes	Uncertain
77	MS	0.137	4.65	0.438	0.136	Yes	Yes	Yes
78	MS	0.319	4.65	0.444	0.164	Yes	No	Uncertain
79	MS	0.201	4.46	0.468	0.161	Yes	Yes	Yes
80	MS	0.209	4.65	0.475	0.161	Yes	No	Uncertain
81	MS	0.361	4.65	0.473	0.179	Yes	Yes	Yes
82	MS	0.147	4.46	0.473	0.153	Yes	Yes	Yes
83	MS	0.233	4.46	0.419	0.148	Yes	Yes	Yes
84	MS	0.159	4.46	0.395	0.129	No	Yes	Uncertain
85	MS	0.263	4.65	0.444	0.158	Yes	Yes	Yes
86	MS	0.051	4.32	0.389	0.103	No	Yes	Uncertain
87	MS	0.157	4.65	0.338	0.108	No	No	No
88	MS	0.247	4.65	0.328	0.115	Yes	No	Uncertain
89	MS	0.205	4.46	0.343	0.118	Yes	Yes	Yes

Table 1 continued

No.	Lithology	*T*	*G*	*R*	*P*	Debris flow[a]	Debris flow[b]	Debris flow[c]
90	MS	0.154	4.65	0.334	0.106	No	No	No
91	MS	0.213	4.65	0.367	0.125	No	No	No
92	MS	0.198	4.65	0.508	0.17	No	No	No
93	MS	0.097	4.65	0.481	0.14	No	No	No
94	MS	0.163	4.65	0.465	0.15	Yes	No	Uncertain
95	MS	0.294	4.65	0.462	0.168	Yes	No	Uncertain
96	MS	0.367	4.46	0.463	0.179	Yes	No	Uncertain
97	MS	0.303	4.46	0.456	0.17	Yes	No	Uncertain
98	MS	0.268	4.65	0.482	0.172	Yes	No	Uncertain
99	MS	0.166	4.65	0.457	0.148	No	No	No
100	MS	0.151	4.65	0.453	0.144	Yes	No	Uncertain
101	MS	0.187	4.65	0.454	0.151	Yes	Yes	Yes
102	MS	0.159	4.46	0.598	0.196	Yes	Yes	Yes
103	MS	0.119	4.65	0.498	0.151	Yes	Yes	Yes
104	MS	0.091	4.65	0.469	0.136	Yes	Yes	Yes
105	MS	0.230	4.65	0.565	0.195	Yes	No	Uncertain
106	MS	0.192	4.65	0.434	0.145	Yes	Yes	Yes
107	MS	0.140	4.65	0.665	0.208	Yes	No	Uncertain
108	MS	0.127	4.65	0.591	0.181	Yes	No	Uncertain
109	MS	0.155	4.65	0.467	0.149	No	No	No
110	MS	0.062	4.65	0.372	0.099	No	No	No
111	MS	0.062	4.65	0.393	0.104	No	No	No
112	MS	0.173	4.65	0.607	0.198	Yes	Yes	Yes
113	MS	0.086	4.65	0.672	0.191	No	No	No
114	MS	0.109	4.65	0.64	0.191	Yes	No	Uncertain
116	MS	0.155	4.65	0.714	0.228	Yes	Yes	Yes
117	MS	0.248	4.65	0.722	0.253	Yes	Yes	Yes
118	MS	0.334	4.65	0.731	0.272	Yes	Yes	Yes
119	MS	0.206	4.65	0.807	0.273	Yes	Yes	Yes
120	MS	0.231	4.65	0.812	0.281	Yes	Yes	Yes
121	MS	0.203	4.65	0.812	0.274	Yes	Yes	Yes
122	MS	0.180	4.65	0.856	0.282	Yes	Yes	Yes
123	MS	0.115	4.65	0.563	0.169	No	Yes	Uncertain

For an explanation see text

Lithology, *T*, *G*, and *R* are data pertaining to the formation (source) area of the gullies

[a] Debris flow judged by Chen (2007)

[b] Debris flow judged by Lin et al. (2003)

[c] Debris flow defined in this paper

[1] EO: Quartz sandstones alternated with hard shales

[2] OM: Hard shales alternated with quartz sandstones

[3] EH: Slates

[4] MS: Siltstones interbedded with shales

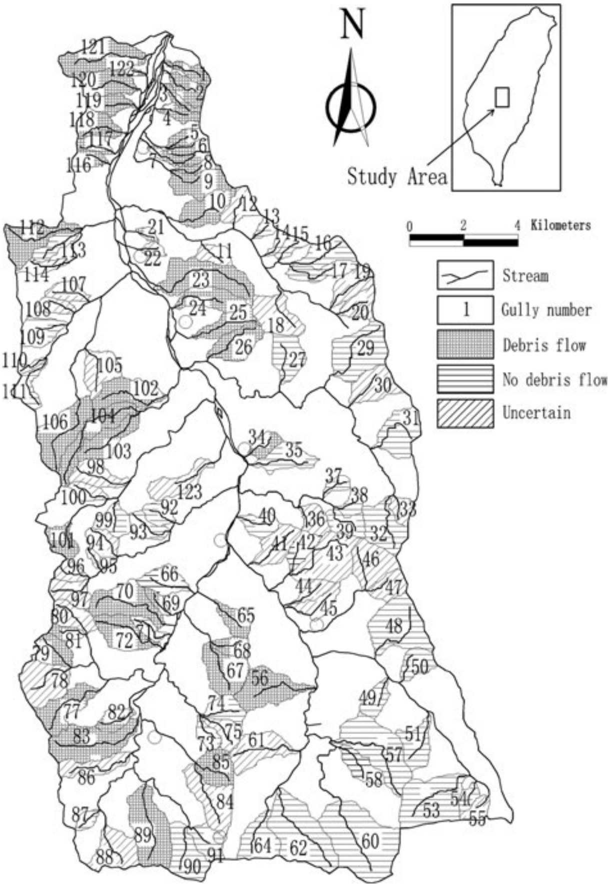

Fig. 1 The investigated gullies in the Chenyulan River Watershed

will focus on the role of topographical factors in the formation (source) section of the catchment. Yu et al. (2011) and Li (2012) obtained a dimensionless topographic factor describing the role of topography in the formation of debris flows with a "fire hose" mechanism:

$$T = FJ\left(A/_{A_0}\right)^{0.2} = J\left(A/_{L^2}\right)\left(A/_{A_0}\right)^{0.2} \tag{1}$$

in which T is the dimensionless topographic factor; F (=A/L^2) is the form factor of the formation section of the gully; J is the average slope of the channel in the formation section of the gully; A is the area of the formation section of the gully (km^2); A_0 is the unit area of the gully (=1 km^2), and L is the stream length in the formation section of the gully (km).

The stream length is determined by accumulating the length of a series of straight line segments along its flow direction. The form factor is calculated as the ratio between the area of the formation section and the square of the stream length in the formation section. The form factor is highly related to the distribution of the hydrograph: a larger form factor produces a larger discharge and velocity than a smaller form factor. Therefore, under the same conditions, a watershed area with a large form factor has a higher likelihood to

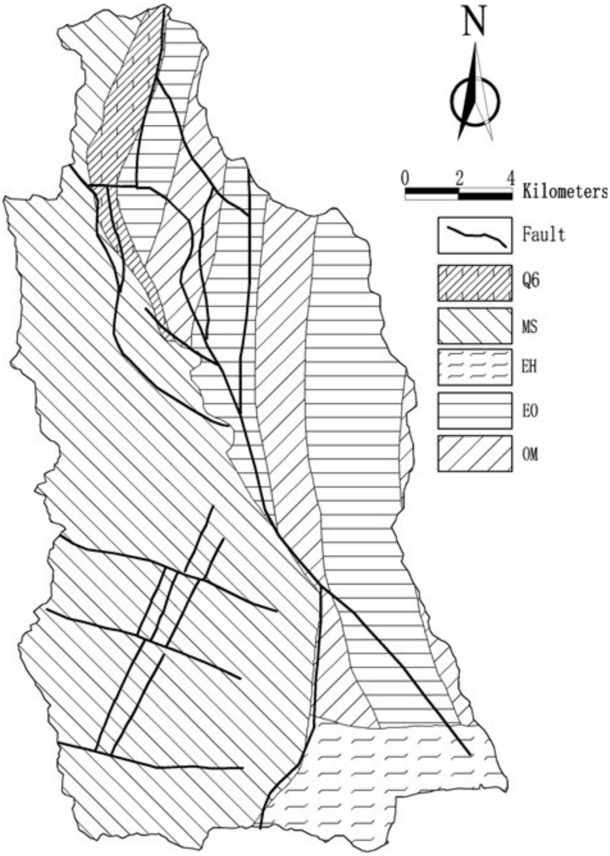

Fig. 2 Geologic setting of Chenyulan River Watershed. *Q6* Alluvium; *MS* Siltstones interbedded with shales; *EH* Slates; *EO* Quartz sandstones alternated with hard shales; *OM* Hard shales alternated with quartz sandstones

generate debris flows (Chang 2007). The average slope of a stream is calculated as the elevation difference between the upslope end of the stream and the outlet of the section, divided by the stream length. These parameters also influence the surface flow discharge and the flow velocity and thus the resulting down slope movement of sediments. The topographic factors are calculated using Google Earth. The values of the topographic factor *T* for all the 117 gullies are listed in Table 1.

3.2 The geological factor

Accumulation of solid material into channels forms the source for the debris flows, which will be triggered by the erosion of flash floods (Wang and Fan 2006; Tan et al. 1994): The harder the rock, the greater the particle size of the solid material, and the longer the accumulation time and thus the more difficult to trigger debris flows. On the other hand, soft rocks have a larger potential to supply solid source material delivered by landslides. The smaller the particle size of solid materials, the faster the deposition of source material, and the easier debris flows are activated (Yu et al. 2012). By using this idea, Yu et al.

Table 2 The classification of rock types by firmness

Lithology	Firmness coefficient F_0
Basalt, quartzite, peridotite, etc.	14
Gabbro, diorite, andesite, etc.	13
Granite, rhyolite, amphibolite, quartz (siliceous) schist, etc.	12
Dolomite, limestone, gneiss, siliceous slate, marble, conglomerate, etc.	10
Quartz schist, sandy (calcareous, carbonaceous) slate, quartz (siliceous) sandstone, etc.	9
Calcarinate, etc.	8
Phyllite, volcanic tuff, aleuvite, etc.	6
Micacite, marlite, dirtysandstone, etc.	5
Shale (mud shale, arenaceous shale), mudstone, etc.	4

(2012) obtained a dimensionless geologic factor to represent the role of geology in the formation of debris flows triggered by flash floods in channels:

$$G = F_0 C_1 C_2 C_3 \tag{2}$$

in which G is the dimensionless geologic factor; F_0 is the average firmness coefficient of the lithology in the formation section of the gully; C_1 is a correction coefficient for seismic intensity in the formation section of the gully; C_2 is a correction coefficient for tectonics (faults); C_3 is the correction coefficient for weathering.

Based on field investigations, the average firmness coefficient for lithology F_0 was revised from the Protodrakonov Coefficient (Protodyakonov 1962) for rock strength (Yu et al. 2012, see Table 2). The values of this coefficient for the 117 gullies are given in Table 2, Figs. 1 and 2. As was mentioned before: four lithological units can be distinguished in the study area: (1) quartz sandstones with alternating hard shales, (2) hard shales with alternating quartz sandstones, (3) slates, and (4) siltstones interbedded with shales. In group (1), two-third consists of quartz sandstones ($F_0 = 9$) and one-third of hard shales ($F_0 = 5$) which gives a weighted average firmness coefficient of $F_0 = 7.67$ for group (1). Two-third in group (2) consists of hard shales ($F_0 = 5$) and one-third of quartz sandstones ($F_0 = 9$). Thus, the weighted average firmness coefficient of group (2) $F_0 = 6.33$. $F_0 = 9$ is the average firmness coefficient for group (3) (slates). The siltstones ($F_0 = 6$) and shales ($F_0 = 4$) are equally distributed in group (4) which delivers a weighted average firmness coefficient $F_0 = 5$. When the lithology in the formation section of a gully belongs to more than one group, the average firmness coefficient of the major group is taken as the average firmness coefficient of the gully. The mean value of the average firmness coefficients of groups is taken when the groups have nearly the same importance. The lithologies for the 117 gullies are listed in Table 1.

The correction coefficients C_1, C_2, and C_3 (see Eq. 2) of, respectively, seismic intensity, tectonics (faults), and weathering for the formation area of the gullies are listed in Table 3 (Yu et al. 2012).

The seismic intensity in the study area is VIII, which gives a correction coefficient C_1 of 0.93 (see Table 3). The correction factor with respect to the tectonics of all the 117 gullies is determined with the Figs. 1 and 2 by counting the faults crossing the formation section of the gullies. The correction factor for the weathering in Table 3 is based on physical weathering. Physical weathering plays an important role in the formation of debris flows:

Table 3 Correction factors for seismic intensity, faults (tectonics), and degree of weathering

Factor\value	1	0.96	0.93	0.90
Seismic intensity C_1	VI and below	VII	VIII	IX and above
Tectonics C_2	No fault	1 fault	2 faults	3 and more faults
Weathering C_3	Mini	Weak	Moderate	Strong

the mechanically damaged and frigid-weathered clasts of blocks form the ideal solid source material. Important for physical weathering are the differences in day and night temperatures around 0 °C, which causes frost splitting of rock material. Rock damages and enlarging cracks are caused by frequently freezing and melting of water in fissures (Fookes et al. 1971). The intensity of weathering is mainly affected by the average annual rainfall and temperature of an area. The intensity of physical weathering is determined not only by the average annual rainfall and temperature but also by lithology. So C_3 and F_0 in Eq. 2 include the temperature and rainfall difference, and lithology for the physical weathering. The average annual rainfall lies in a range between 1,858 and 3,912 mm, and the average annual temperature varies between 15 and 24 °C in the study area. Thus, the coefficient C_3

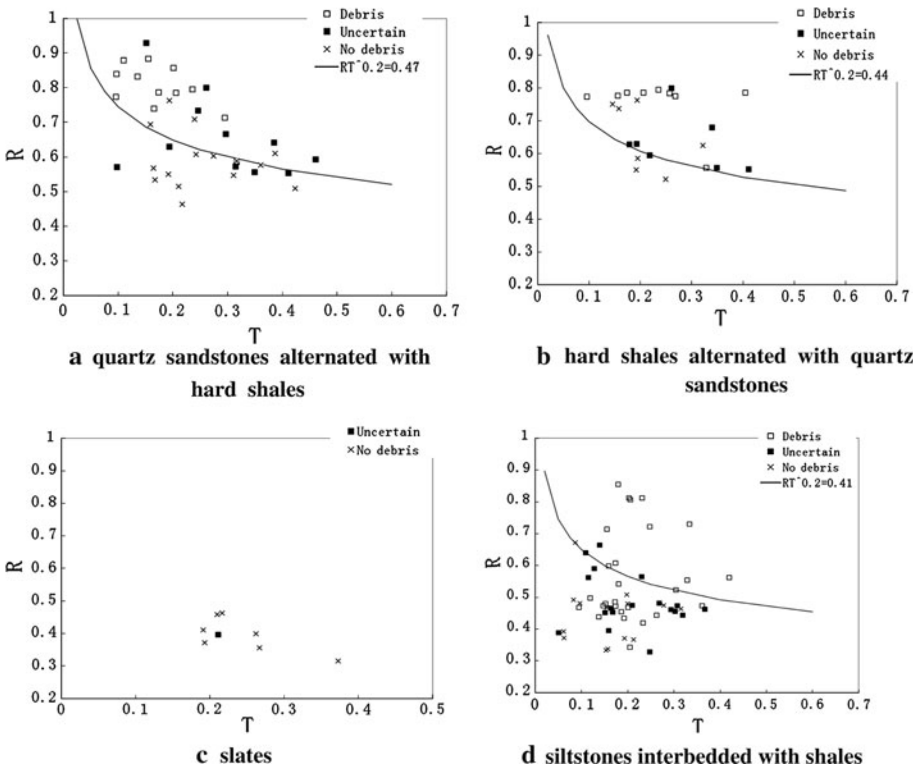

Fig. 3 Relationship of the topographic factor T and the hydraulic factor R for areas with different lithology. **a** Quartz sandstones alternated with hard shales. **b** Hard shales alternated with quartz sandstones. **c** Slates. **d** Siltstones interbedded with shales

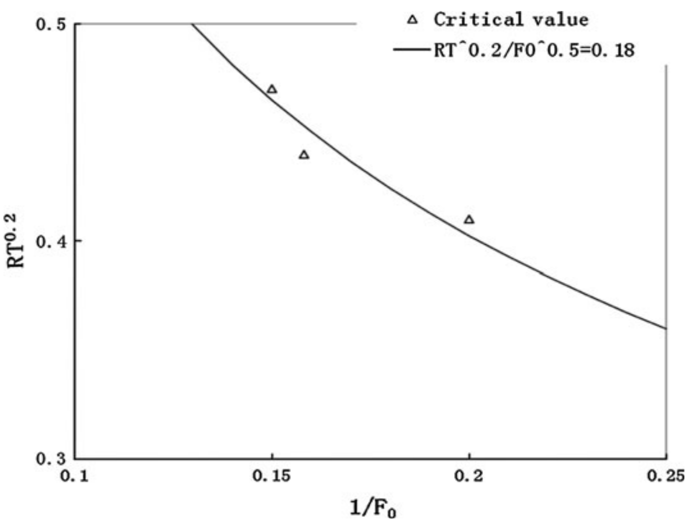

Fig. 4 Relationship of $RT^{0.2}$ and $1/F_0$

in the research area is 1 according to Fookes et al. (1971). The resulting final geologic values for G for all the 117 gullies are listed in Table 1.

3.3 The hydrological factor

The hydraulic triggering conditions are narrowly related to the rainfall characteristics. Therefore, in this paper, we use the rainfall characteristics instead of the hydraulic conditions, which are difficult to assess. Short-duration high-intensity rainfall is the main triggering factor for the gully type debris flows in the Chenyulan River Watershed during Typhoon Toraji. Shieh et al. (2009), Wu et al. (1990), and Tan and Han (1992) used the 1-h

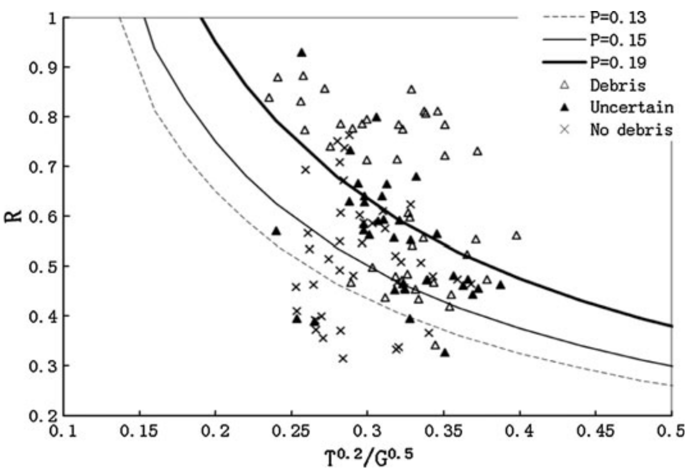

Fig. 5 Formation model showing probability fields for the occurrence of debris flows induced by the Typhoon Toraji in the Chenyulan River Watershed

Table 4 The probability areas of debris flow occurrence distinguished by Eq. 5

Probability area	No debris flows		Debris flows		Uncertain	
	Number	%	Number	%	Number	%
Very low	12	30	1	2.3	4	11.8
Low	7	17.5	4	9.3	4	11.8
Medium	15	37.5	11	25.6	18	52.9
High	6	15	27	62.8	8	23.5

or 10-min rainfall intensity and effective cumulative precipitation to predict the debris flows with a "fire hose" mechanism. The critical rainfall can be expressed as:

$$S = B + KI \tag{3}$$

in which S is the critical rainfall (mm); B is effective cumulative precipitation, the rainfall until the start of the debris flow (mm); K (h or min.) is the coefficient of rainfall intensity; I is the rainfall intensity per 1 h or 10 min (mm/h, or mm/10 min).

Wu et al. (1990) indicated that the 10-min rainfall intensity is strongly correlated with the triggering of debris flows with a "fire hose" mechanism. Also in some cases, 1-h rainfall intensities show a relationship with the formation of debris flows like the Zhouqu event in China (Yu et al. 2010). However, 10-min intensities show better correlations with debris flow initiation. Unfortunately, only 1-h rain intensities are available in the study area. So, for the hydrological factor, we have to use the 1-h intensity.

Shieh et al. (1995) analyzed the critical rainfall with 1-h intensities triggering debris flows and obtained a K-value (Eq. 3) for the coefficient of rainfall intensity $K = 38.5$ in eastern Taiwan before 1995, but a K-value of 10.5 in the central area of Taiwan after the Chi–Chi earthquake in 2000–2001 (Shieh 2001). Jiang and Lin (1991) obtained K values between 179 and 16.7 in different area of Taiwan during the 1980s. Fan and Yao (1997) found a K-value of 10.2 in eastern Taiwan before 1996, and Tan (1991) pointed out that the K-coefficient was 4.1 in the mainland of China during the period 1975–1985. Jan et al. (2002) obtained a K-value of 10 for the central area of Taiwan in the period 2000–2002 after the Chi–Chi earthquake. So these empirical analyses revealed a large range for the coefficient of rainfall intensity K varying between 4.1 and 179. For the Chi–Chi earthquake affected area, the K-coefficient lies within a smaller range between 10 and 13.7 (I in Eq. 3 is the rainfall intensity per hour in this case) (Shieh 2001; Shieh et al. 2009; Jan et al. 2002). After 7 years of observations at two sites, Shieh et al. (2009) obtained coefficient values of 11.3 and 13.7, respectively. In this study, the coefficient of rainfall intensity K is taken as the average of these two values: 12.5. The cumulative rainfall and 1-h maximum rainfall for each of the 117 gullies are obtained by interpolation of the spatial distribution over the area of the cumulative rainfall and 1-h maximum rainfall given by Chen (2007). Chou et al. (2002) pointed out that in Taiwan between 1981 and 2000, 77 % of the debris flows occurred about half way the duration of the rainfall. Since we do not know the effective cumulative precipitation (B in Eq. 3), we consider half of the cumulative rainfall as the effective cumulative precipitation. The critical rainfall S of the 117 gullies could then be calculated with Eq. 3.

Aleotti (2004) used the annual precipitation to normalize the critical rainfall. This kind of normalization is very important because rainfall values vary widely between the different areas. The difference may be reduced by introducing a normalization with the annual precipitation. Because of the scarcity of rainfall data in the research area during the Typhoon Toraji, the annual precipitation was the only option to normalize the critical rainfall. The normalized critical rainfall (Aleotti 2004) is used for the dimensionless hydraulic (rainfall) factor (Eq. 4):

$$R = {}^{S}\!/_{R_0} = (B + KI)/R_0 \tag{4}$$

in which R is the dimensionless hydraulic (rainfall) factor; R_0 is the annual precipitation of the site (mm). The annual precipitation R_0 for each gully is obtained from the spatial distribution of annual rainfall in the study area. The values of the hydraulic factor R for all the 117 gullies are listed in Table 1.

4 The formation model for debris flows

The formation conditions for debris flows in the Chenyulan River Watershed during the Typhoon Toraji can now be expressed by the topographic factor T, the geological factor F, and the rainfall factor R. In order to arrive at one single factor for the formation of debris flows, the relation field between these three factors for gullies with debris flows and no debris flows needs to be analyzed. First, the areas with the same lithology are chosen to study the relation field between factor T and factor R for gullies with debris flows and no debris flows. Figure 3 shows the scatter plot of the gullies with debris flows and no debris flows (including the uncertain observations) for the four lithological units. Apart from the uncertain cases, gullies with debris flows and no debris flows can be found in three out of four lithological units: group (1) (quartz sandstones alternated with hard shales), group (2) (hard shales alternated with quartz sandstones), and group (4) (siltstones interbedded with shales). In gullies belonging to group (3) (slates), no certain debris flows were found. For the groups (1), (2), and (4), the function $RT^{0.2} = C$ (C is a constant) made an optimal distinction between debris flow and no debris flows. In Fig. 3a, b, the critical lines described with $RT^{0.2} = 0.47$ and 0.44, respectively, can divide all "debris" from most of the "no debris" cases. In Fig. 3d, the critical line described with $\mathrm{RT}^{0.2} = 0.41$ divides a large part of "debris" from all cases of "no debris". So a first exponential graph with T and R ($\mathrm{RT}^{0.2}$) could be obtained, separating more or less debris flows from no debris flows for three lithological units.

The average firmness coefficients F_0 of the three lithological groups (4), (2), and (1) are 5, 6.33, and 7.67, respectively (see section "Geological factor"). Now one can set up a relationship between the critical values $RT^{0.2} = 0.41$, 0.44, 0.47, and the average firmness coefficients for the three lithological units. The graph can be described with the function $RT^{0.2}/F_0^{0.5} = 0.18$ by regression analysis, ($R^2 = 0.86$), which makes a reasonable fit with the 3 critical values (see Fig. 4). The formation factor P can be obtained from this relationship between T, G, and R (Eq. 5):

$$P = {}^{RT^{0.2}}\!/_{G^{0.5}} \geq C_r \tag{5}$$

in which P is the formation factor; C_r is a critical value for the formation of debris flows.

The formation factor P for all the 117 gullies is listed in Table 1. Figure 5 shows a scatter plot of R against $T^{0.2}/\mathrm{G}^{0.5}$ (from Eq. 5) for all the 117 gullies and three graphs for three different values of P: marking three critical probability values for debris flow formation: $C_{r1} = 0.13$, $C_{r2} = 0.15$, and $C_{r3} = 0.19$. These critical values deliver a division into four classes of the probability of debris flow occurrence. Debris flows are hardly formed in the area with $P < C_{r1}$. This area can be considered as a *very low probability* or safe area. Few debris flows are formed in the area between $0.13 \leq P < 0.15$, which is a *low probability* area where one has to watch out. Some debris flows are formed in the area between $0.15 \leq P < 0.19$, which makes this area a *medium probability* or an alarm area. When $P \geq 0.19$, debris flows are triggered in most gullies, which makes it a *high probability* area. In this area, people have to be evacuated to safer places. Table 4 shows the number and percentages of debris flows and no debris flows for the different classes distinguished by Eq. 5. There is 1 debris flow (2.3 % of all debris flows) and there are 12 no debris flows (30 % of all no debris flows) in the safe area class. There are 27 debris flows (62.8 % of all debris flows) and 6 no debris flows (15 % of all no debris flows) in the *high probability* class.

Equation 5 shows that the hydraulic factor R has the largest influence on the formation factor P compared to the other two factors. The exponential values of G and T are 0.5 and 0.2, respectively. Therefore, the geological factor G is more important than the topographic factor T. This is why in many studies only the hydraulic factors are used empirically to analyze the occurrence of debris flows.

5 Discussion

In 2001, the Typhoon Toraji provided an unprecedented amount of data for studying the formation of debris flows with a so-called "fire hose" mechanism in the Chenyulan River Watershed. With the lack of a detailed field survey, some mistakes are made by two studies using only SPOT images to determine the occurrence of debris flows in this area. The category "uncertain" for the occurrence of debris flows is added in this study to account for the difference in judgment between the two studies.

Neglecting the impact of the uncertain cases in the results, the distinction between occurrence and no occurrence of debris flows by means of the formation factor P is acceptable despite the fact that one debris flow occurred in the area with very low probability and 6 gullies with no debris flows are found in the area with very high probability. However, the uncertainty in the detection of debris flows may affect the result of the formation model, and the hypothesis of a "fire hose" mechanism for all the gullies is also another source of errors.

The study area experienced 400–600 cm/s^2 of ground acceleration during the Chi–Chi earthquake, which significantly decreased the triggering threshold for debris flows. In this study, the effect of the Chi–Chi earthquake is assumed to be the same all over the area. This may also form a source of errors for the judgment of the formation of debris flows with the formation factor P. The rainfall threshold for debris flows recovered gradually in subsequent years after the earthquake but is still lower than the original threshold before the earthquake. So the critical value C_r in Eq. 5 will increase in the subsequent years after the Typhoon Toraji. Future investigations of the influence of earthquakes on the change of the critical value with the years are needed.

The evaluation of F_0, C_1, C_2, and C_3 was supported by some field investigations and verified by some references (Yu et al. 2012). But a multiplication of these four factors as presented in Eq. 2 may be not the best solution although it works quite well in some areas. Future investigations on analysis of the relationships among these factors are needed.

Landslides, channel bed erosion, and destruction of natural dams are three common causes that trigger debris flows (Takahashi 2000). In this study area, only the "fire hose" mechanism (channel bed erosion) is considered as the trigger mechanism of debris flows in the study area. The formation factor P is not suitable for the other mechanisms of debris flow formation like landslides and natural dam breaks which occurred during the Typhoon Herb, the Typhoon Midulle, and the Typhoon Morakot.

In this study, only 5 lithologies were involved in the determination of the geological factor. The applicability of the geological factor in other areas is an important subject for the future research. The relationship between $RT^{0.2}$ and F, and the function $P = RT^{0.2}/G^{0.5}$ is based on only 3 points (see Fig. 4). Future work with a larger number of lithological classes is needed to test the relationship between R, T, and G.

The critical value C_{r3} is 46 % higher than the critical value C_{r1}, which shows a moderate performance of the formation model. For a more accurate prediction of the occurrence of debris flows, more research is needed to reduce the difference between C_{r1} and C_{r3}.

6 Conclusions

The Typhoon Toraji, which occurred 2 years after Chi–Chi earthquake caused a severe debris flow activity in the Chenyulan River Watershed. Short-duration high-intensity rainfall was the main inducing factor for these gully type debris flows with a “fire hose” mechanism. This research proposed a formation model for debris flows based on a topographic, geological, and hydraulic factor. The type of these dimensionless factors is not deduced from the statistic analyses of a given area but based on the mechanism for the formation of debris flows. The formation model has a general nature and can be used in other areas, despite the fact that the formation factor P is based in this study on a statistical analyzes of the Chenyulan River basin.

With the combination of the topographic, geological, and hydraulic factor, a formation factor was obtained which delivered a good judgment of the occurrence of debris flows in the study area. In our view, the formation model offers a new and exciting way to forecast the probability of occurrence of debris flows with a “fire hose” mechanism. However, to improve the understanding of the occurrence and triggering mechanisms of debris flows, and for a better understanding of the long-term impact of earthquakes on the spatial and temporal frequency of debris flows, future research is needed to determine the set of errors in mapping debris flows with SPOT images, the change in critical probability values after successive years, and to reduce the difference between critical probability values.

Acknowledgments This work was supported by The National Nature Science Foundation of China (NSFC, contract number: 40871054) and The State Key Laboratory of Geohazard Prevention and Geoenvironment Protection Foundation (contract number: SKLGP2010Z004). We especially like to thank Hsien-Ter Chou and Su-Chin Chen for their suggestions and providing information. We thank the reviewers for their comments that helped us to greatly improve the presentation of this work. We are grateful to Dr. Theo van Asch for having provided a very helpful review of the manuscript and for help on the English editing of the manuscript.

References

Akgun A, Dag S, Bulut F (2008) Landslide susceptibility mapping for a landslide-prone area (Findikli, NE of Turkey) by likelihood-frequency ratio and weighted linear combination models. Environ Geol 54:1127–1143

Aleotti P (2004) A warning system for rainfall-induced shallow failures. Eng Geol 73:247–265

Bai HJ (2007) The research of knowledge expression on debris-flow potential analysis by using rough sets theory—a case study of Chen-Yu-Lan stream. Master thesis of Feng Chia University, pp 1–88 (in Chinese with English abstract)

Cannon SH, Gartner JE, Rupert MG, Michael JA, Rea AH, Parrett C (2010) Predicting the probability and volume of postwildfire debris flows in the intermountain western United States. Geol Soc Am Bull 122(1–2):127–144

Catani F, Casagli N, Ermini L, Righini G, Menduni G (2005) Landslide hazard and risk mapping at catchment scale in the Arno River basin. Landslides 2:329–342

Chang TC (2007) Risk degree of debris flow applying neural networks. Nat Hazards 42:209–224

Chang TC, Chao RJ (2006) Application of back-propagation networks in debris flow prediction. Eng Geol 85:270–280

Chang TC, Chien YH (2007) The application of genetic algorithm in debris flows prediction. Environ Geol 53:339–347

Chen X (2007) Evaluation on the occurrence frequency of debris flow in the Chenyulan River watershed. Master thesis of Chang Jung Christian University, pp 1–73 (in Chinese with English abstract)

Chen WF, Li YH, Wu HL (2005) Study of judging debris flow occurrence by combing the physiographical factors and rainfall condition—Chen-Yu-Lan stream watershed as an example. J Taiwan Geogr Inf Sci 2:27–44 (in Chinese with English abstract)

Chen SC, Chen S, Wu CH (2012) Characteristic of the landslides in Shenmu watershed in Nantou County. J Chin Soil Water Conserv 43(3):214–226 (in Chinese with English abstract)

Chou HT, Liaw WM, Yao SW (2002) Threshold conditions for rainfall-induced debris flows. J Chin Civil Hydraul Eng 14(1):1–8 (in Chinese with English abstract)

Coe JA, Glancy PA, Whitney JW (1997) Volumetric analysis and hydrologic characterization of a modern debris flow near Yucca Mountain Nevada. Geomorphology 20:11–28

Fan JH, Yao ZS (1997) A preliminary study on hydrologic and physiographic criteria of debris flow in the east Taiwan Tainan. Conference of agriculture engineering in 1997, Tainan, pp 525–531 (in Chinese)

Fookes PG, Dearman WR, Franklin JA (1971) Some engineering aspects of rock weathering with field examples from Dartmoor and elsewhere. Q J Eng Geol 4(3):161–163

Godt JW, Coe JA (2007) Alpine debris flows triggered by a 28 July 1999 thunderstorm in the central Front Range, Colorado. Geomorphology 84:80–97

Griffiths PG, Webb RH, Melis TS (2004) Frequency and initiation of debris flows in Grand Canyon, Arizona. J Geophys Res 109:F04002 http://dx.doi.org/10.1029/2003JF000077

Huang R, Li W (2009) Fault effect analysis of Geo-Hazard triggered by Wenchuan earthquake. J Eng Geol 18(4):437–444 (in Chinese with English abstract)

Jan CD, Chen CL (2005) Debris flows caused by Typhoon Herb in Taiwan. In: Jakob M, Hungr O (eds) Debris-flow hazards and related phenomena. Springer, Berlin, pp 539–564

Jan CD, Lee MH, Chen JQ (2002) Research on the reliability of discharge of debris flows. Conference of supplement research plan in the management of emergent slope hazards in 2002, pp 251–273 (in Chinese)

Jiang YZ, Lin QY (1991) Analysis on the rainfall characteristics of occurrence of debris flows. J Chin Soil Water Conserv 22(2):21–37 (in Chinese with English abstract)

Johnson AM, Rodine JR (1984) Debris Flow. In: Brunsden D, Prior DB (eds) Slope Instability. John Wiley and Sons Ltd., Chichester, pp 257–361

Kaima TW, Wang WN, Sguzui H (2000) The landslide disaster induced by the Taiwan Chi–Chi earthquake of 21 September 1999. Landslide News 13:8–12

Lan HX, Zhou CH, Wang LJ, Zhang HY, Li RH (2004) Landslide hazard spatial analysis and prediction using GIS in the Xiaojiang watershed, Yunnan, China. Eng Geol 76:109–128

Lee MH (2006) A rainfall-based debris-flow warning analysis and its application. PHD thesis of National Cheng Kung University, pp 1–229

Lee S, Pradhan B (2007) Landslide hazard mapping at Selangor, Malaysia using frequency ratio and logistic regression models. Landslides 4:33–41

Li L (2012) Study on the topographic factor of gully-type debris flows in strong earthquake areas. Master thesis of Chengdu University of Technology, pp 1–82

Lin CY (2009) Effect of topographic factors on the occurrence of debris flow—take the Chen-yu-lan Creek watershed as an example. Thesis of National Chung Hsing University, pp 1–68

Lin JY, Hung JC, Yang MD (2002) Assessing debris-flow hazard in a watershed in Taiwan. Eng Geol 66:295–313

Lin CW, Shieh CL, Yuan BD, Chieh TC, Liu CH, Lee SY (2003) Impact of Chi–Chi earthquake on the occurrence of landslides and debris flows: example from the Chenyulan river watershed, Taiwan. Eng Geol 71:49–61

Liu C, Dong J, Peng Y, Huang H (2009) Effects of strong ground motion on the susceptibility of gully type debris flows. Eng Geol 104(3–4):241–253

Lopez JL, Perez D, Garcia R (2003) Hydrologic and geomorphologic evaluation of the 1999 Debris flow event in Venezuela. In: 3rd international conference on debris-flow hazards, mitigation: mechanics, prediction, and assessment, Davos, Switzerland, Sept. 13–15, 2003

Lu GY, Chiu LS, Wong DW (2007) Vulnerability assessment of rainfall-induced debris flows in Taiwan. Nat Hazards 43:223–244

Ohlmacher GC, Davis JC (2003) Using multiple logistic regression and GIS technology to predict landslide hazard in northeast Kansas, USA. Eng Geol 69:331–343

Protodyakonov MM (1962) Mechanical properties and drillability of rocks. In: Proceedings of the fifth symposium on rock mechanics. University of Minnesota, Minneapolis, pp 103–18

Ranjan KD, Shuichi H, Atsuko N, Minoru Y, Takuro M, Katsuhiro N (2004) GIS-based weights-of-evidence modelling of rainfall-induced landslides in small catchments for landslide susceptibility mapping. Environ Geol 54:311–324

Shieh CL (2001) Primary study on the hazards standard of debris flow during the Typhoon Toraji. In: Symposium of conference on debris flow hazards and mitigation, Chengdu, pp 83–102 (in Chinese)

Shieh CL, Luh YC, Yu PS, Chen LJ (1995) The critical line of debris flow occurrence. J Chin Soil Water Conserv 26(3):167–172 (in Chinese with English abstract)

Shieh CL, Chen YS, Tsai YJ (2009) Variability in rainfall threshold for debris flow after the Chi–Chi earthquake in central Taiwan, China. Int J Sediment Res 24:177–188

Takahashi T (2000) Initiation and flow of various types of debris flow. In: Wieczorek GF, Naeser ND (eds) Debris-flows hazard mitigation: mechanics, prediction, and assessment. Balkema, Rotterdam, pp 15–25

Tan W (1991) Research on the rainfall threshold of debris flow. In: Symposium of second national conference of debris flow, Chengdu, pp 136–142 (in Chinese)

Tan W, Han Q (1992) Research on the critical rainfall of debris flows in Sichuan Province. China. Hazards 7(2):37–42 (in Chinese with English abstract)

Tan W, Wang C, Yao L (1994) Regional prediction of debris flow and landslide on heavy rainfall—in the Panxi Area, Sichuan, China, Chengdu, Sichuan Sciences Press, pp 8–11 (in Chinese)

Tiranti D, Bonetto S, Mandrone G (2008) Quantitative basin characterisation to refine debris-flow triggering criteria and processes: an example from the Italian Western Alps. Landslides 5:45–57

Tunusluoglu MC, Gokceoglu C, Nefeslioglu HA, Sonmez H (2008) Extraction of potential debris source areas by logistic regression technique: a case study from Barla, Besparmak and Kapi mountains (NW Taurids, Turkey). Environ Geol 54:9–22

VanDine DF (1985) Debris flow and debris torrents in the Southern Canadian Cordillera. Can Geotech J 22:44–68

Wang S, Fan X (2006) The Hazards and engineering control of low frequency debris flow. J Mt Sci 24(5):562–568 (in Chinese with English abstract)

Wu J, Kang Z, Tian L, Zhang S (1990) Observation and research on the debris flows in Jiangjia Gully, Yunnan Province, China. Science Press, Beijing, pp 197–221

Yu B, Yang Y, Su Y, Huang W, Wang G (2010) Research on the giant debris flow hazards in Zhouqu County, Gansu Province on August 7, 2010. J Eng Geol 18(4):437–444 (in Chinese with English abstract)

Yu B, Li L, Ma Y, Zhang J, Wu Y, Zhang H, Chu S, Qi X (2011) Research on topographical factors in the formation of gully type debris flows. River, coastal and estuarine morphodynamics: RCEM2011. Tsinghua University Press, Beijing, pp 1–10

Yu B, Chu S, Lu K, Han L, Xie H (2012) A study about the relationship between the frequency of debris flows and lithology. In: Eberhardt et al. (eds) Landslides and engineered slopes: protecting society through improved understanding. Taylor & Francis Group, London, pp 757–761